An anisotropic band model for helimagnetism and spin-density waves, with application to Cr and MnP

1990 J. Phys.: Condens. Matter 2 4637

(http://iopscience.iop.org/0953-8984/2/20/010)

J. Phys.: Condens. Matter 2 (1990) 4637–4654. Printed in the UK

An anisotropic band model for helimagnetism and spin-density waves, with application to Cr and MnP

J Sjöström
Department of Theoretical Physics, Royal Institute of Technology, S-100 44 Stockholm, Sweden

Received 30 October 1989

Abstract. An expression for a general q-dependent static spin susceptibility is derived by means of perturbation theory, including a two-electron exchange operator and spin–orbit coupling. Numerical calculations for hypothetical sets of two bands close to the Fermi level show that significantly stronger magnetic response can occur for $q \neq 0$ than for $q = 0$, but only for interband transitions and if the bands intersect the Fermi surface in such a way that the region of close contact between the q-shifted bands and the Fermi surface is larger than the corresponding area for the unshifted bands. According to performed band calculations, this can be the case for Cr (spin-density wave, SDW) and MnP (helix). A symmetry consideration of a helical spin distribution shows that the symmetric and antisymmetric parts of the anisotropic exchange correspond to different bunching and modulation of the spins. For example, a longitudinal SDW (as in Cr) corresponds to a vanishing antisymmetric exchange (AE), while a circular uniform helix minimises the AE and has a vanishing non-diagonal symmetric exchange.

1. Introduction

The first report of a magnetic structure with helical spin (HS) arrangement is from 1958 by Nagamiya for MnO_2 [1]. Earlier observations of the neutron diffraction spectrum of MnO_2, which had given puzzling results, gave support to the interpretation that the magnetic moments change direction periodically like a helix incommensurate with the lattice. At the same time Carliss *et al* [2] found that the magnetic structure of Cr is a complicated type of antiferromagnet where all the magnetic moments have the same direction while their magnitude is sinusoidally modulated, i.e. described by a spin-density wave (SDW).

As the experimental methods were refined and the number of investigated magnetically ordered systems increased, the number of systems discovered with helical structures and other complex types has increased. A compilation (table 1) by the author shows, however, that incommensurate magnetic structures are still uncommon compared with the large number of systems with collinear structures.

In a localised spin model based on the Heisenberg Hamiltonian, it has been established that positive exchange integrals correspond to ferromagnetism and negative to antiferromagnetism. A necessary, but not sufficient, condition for a helix, in general incommensurate with the lattice, is that exchange integrals of different sign occur [1, 3].

0953-8984/90/204637 + 18 $03.50

By using molecular field theory or other statistical methods, one may also treat itinerant magnetic systems at arbitrary temperatures. However, such methods have the drawback that they give almost no fundamental information about the exchange since the magnetic field is introduced *ad hoc*.

In the 1960s several papers were published which treated the spin-density wave in Cr in an electron-gas approach, where the spins were polarised by the exchange interaction. The results can be summarised in the following way: (i) In the Hartree–Fock theory, instabilities in the calculated susceptibility curve occurred at $q = 2k_F$ [4]. (ii) The instabilities occurred only for long-range interaction with a lower electron density than for realistic metals [5]. (iii) The Fermi surface is crossed by several 3d bands [6]. (iv) Two nearby bands, whose energies are close to each other and the Fermi surface, lead to an instability of the spin susceptibility for a small q vector [7]. The only paper from the 1960s which we have found to be a basis for a more general theory for HS and SDW is the band theoretical part of the work of Fedders and Martin [7], where they used the T matrix for electron–hole scattering in a two-band theory. However, that paper was adapated to explain the SDW in Cr and is not applicable to HS since spin–orbit interaction is neglected.

More recently Ukai and Mori [8] performed band calculations for Cr by introducing potentials corresponding to a lower symmetry than that of the crystal. They found, in agreement with experimental results, that a SDW with wavelength of 21 times the lattice constant gave the lowest energy.

Kataoka *et al* [9] used perturbation theory to derive an expression for a q-dependent susceptibility in an itinerant system including spin–orbit coupling. They found, for example, that the spin–orbit coupling by means of the antisymmetric part of the susceptibility tensor can be important for establishing a helix. However, that work is based on a one-band approach. As we will argue, and as has been found by Fedders and Martin [7], intraband excitations can give rise to a helix or SDW only under not very realistic conditions. In a real metal there exist multiple bands and mixings between different bands, which furthermore intersect each other at several points. A necessary feature of a physically reasonable theoretical model of itinerant magnetism is thus that it takes into account interband transitions as well as the spin–orbit coupling. As far as we know, no such model has been developed for incommensurate magnetism.

One way to circumvent the difficulties discussed above is to use density-functional theory. Kübler *et al* [10] have, for non-collinear antiferromagnetism, very recently performed a self-consistent spin-polarised band calculation based on the local approximation. A generalisation of their method to incommensurate structures seems to be possible but leads to very complicated computational problems and as far as we know only cluster calculations [11, 12] and non-self-consistent band calculations [13] have been performed for HS. We believe that self-consistent band-structure calculations with a reasonable approximation for the potential is the best method to determine the energies for different magnetic structures for a given system. However, if one is mainly interested in the fundamental physical principles of incommensurate magnetism, it seems that an appropriate investigation of a general spin-propagation-vector-dependent susceptibility should give more relevant information. We will therefore in this paper generalise the work by Kataoka *et al* [9] to include a two-electron exchange operator, which enables transitions between different band electrons (sections 2, 3 and 5). By utilising symmetry arguments, we obtain in section 4 some characteristic properties for HS and SDW. In section 6 we make a simple application to MnP (helix) and Cr (SDW).

2. Hamiltonian for two-band electrons in a crystal

In order to study the magnetic energy in a multi-phase magnetically ordered system the q-dependent susceptibility tensor $\chi(q)$ is a very useful quantity since its maximum value corresponds to the lowest exchange energy. A peak in $\chi(q)$ at $q = 0$ would then mean ferromagnetism, and the one at some other q would indicate a helix, SDW or a more complicated arrangement of the magnetic moments and with a period defined by that wavevector $\boldsymbol{q}$.

In order to derive a general q-dependent susceptibility for a two-band system we consider the following effective Hamiltonian in second quantisation:

$$\mathcal{H} = \mathcal{H}_0 + \mathcal{H}_{ex} + \mathcal{H}_{so}. \tag{1}$$

Here $\mathcal{H}_0$ is the Hamiltonian for the non-magnetic system without the spin–orbit coupling. It includes, for example, the total kinetic energy of the system and core–electron interaction and is a diagonal operator given by

$$\mathcal{H}_0 = \sum_k \varepsilon_k \sum_s a^+_{ks} a_{ks'}. \tag{2}$$

Further, in (1) $\mathcal{H}_{ex}$ is an effective operator, which represents the excess exchange energy for all possible two-electron excitations that arise under spin polarisation of the band electrons. The one-electron processes can be included in $\mathcal{H}_{ex}$ (two independent one-particle processes) and in $\mathcal{H}_0$ (excitation of higher order). In second quantisation $\mathcal{H}_{ex}$ has the general form

$$\mathcal{H}_{ex} = \frac{1}{2} \sum_{k_1,s_1} \sum_{k_2,s_2} \sum_{k_3,s_3} \sum_{k_4,s_4} X_{k_3s_3,k_4s_4,k_1s_1,k_2s_2} a^+_{k_4s_4} a^+_{k_3s_3} a_{k_2s_2} a_{k_1s_1}. \tag{3}$$

The matrix element of $\mathcal{H}_{ex}$ is the matrix element of an operator $T_{ex}(x_1, x_2)$ with respect to spin orbitals indicated as subscript

$$\begin{aligned} X_{(k-q)s'',(k'+q)s''',ks,k's'} &= \langle (k-q)s'', (k'+q)s''' | T_{ex} | k's', ks \rangle \\ &= \int \mathrm{d}r_1 \, \mathrm{d}\zeta_1 \, \mathrm{d}r_2 \, \mathrm{d}\zeta_2 \, \Phi^*_{k-q}(r_1) s''(\zeta_1) \Phi^*_{k'+q}(r_2) \\ &\quad \times s'''(\zeta_1) T_{ex}(x_1, x_2) \Phi_{k'}(r_2) s'(\zeta_2) \Phi_k(r_1) s(\zeta_1). \end{aligned} \tag{4}$$

Here we consider the case when two particles in state (k, s) and (k', s') are annihilated and two new particles in the states $(k - q, s'')$ and $(k' + q, s''')$ are created. We use the notation $\Phi_k(r)s(\zeta)$ for the spin orbitals used as basis functions for a_{ks}.

In principle one could start with an operator $T_{ex}(x_1, x_2)$ that has the most general form possible, i.e. it depends in some unspecified way on $x_i = (r_i, \zeta_i)$. Since the spin space is spanned by only two functions, α and β, we can write

$$\begin{aligned} T_{ex}(x_1, x_2) &= T^{\alpha\alpha}_{ex} \alpha(\zeta_1)\alpha(\zeta_2) + T^{\alpha\beta}_{ex} \alpha(\zeta_1)\beta(\zeta_2) + T^{\beta\alpha}_{ex} \beta(\zeta_1)\alpha(\zeta_2) + T^{\beta\beta}_{ex} \beta(\zeta_1)\beta(\zeta_2) \\ &= (\alpha \quad \beta) \begin{pmatrix} T^{\alpha\alpha}_{ex} & T^{\alpha\beta}_{ex} \\ T^{\beta\alpha}_{ex} & T^{\beta\beta}_{ex} \end{pmatrix} \begin{pmatrix} \alpha \\ \beta \end{pmatrix} \end{aligned} \tag{5}$$

if $T_{ex}(x_1, x_2)$ is only a multiplicative linear operator. In the more general case when $T_{ex}(x_1, x_2)$ is a non-multiplicative linear operator, we can write it as a combination of

operators working on r_1 and r_2 and a combination of the vectors of Pauli spin matrices σ_1 and σ_2, i.e.

$$\boldsymbol{T}_{ex}(x_1, x_2) = \sum_{i,j=1}^{3} \sigma_i(\zeta_1)\boldsymbol{T}_{ex,ij}(\boldsymbol{r}_1, \boldsymbol{r}_2)\sigma_j(\zeta_2) \tag{6}$$

so that

$$\boldsymbol{X}_{(\boldsymbol{k}-\boldsymbol{q})s'',(\boldsymbol{k}'+\boldsymbol{q})s''',\boldsymbol{k}s,\boldsymbol{k}'s'} = \sum_{i,j=1}^{3} \langle s''|\sigma_i|s\rangle\langle(\boldsymbol{k}-\boldsymbol{q})s'',(\boldsymbol{k}'+\boldsymbol{q})s'''|\boldsymbol{T}_{ex,ij}|\boldsymbol{k}s,\boldsymbol{k}'s'\rangle\langle s'''|\sigma_j|s'\rangle. \tag{7}$$

The second-order tensor $\boldsymbol{T}_{ex}$ can be separated into a scalar T_{IS}, an antisymmetric vector $\boldsymbol{T}_{AV}$ and a traceless symmetric tensor Φ [3]

$$T_{ex} = T_{IS} + T_{AV} + \Phi \tag{8}$$

where

$$T_{IS} = \tfrac{1}{3}\mathrm{tr}\,\boldsymbol{T}_{ex}$$

$$\boldsymbol{T}_{AV} = \sum \tfrac{1}{2}(T_{ij} - T_{ji})(\boldsymbol{e}_i \times \boldsymbol{e}_j)$$

$$\Phi = \begin{cases} \tfrac{1}{2}(T_{ij} + T_{ji}) & i \neq j \\ T_{ii} - \tfrac{1}{3}\mathrm{tr}\,\boldsymbol{T}_{ex} & (i,j = x,y,z) \end{cases}$$

and $\boldsymbol{T}_{AV}$ (antisymmetric) and Φ (symmetric) correspond to anisotropic exchange and are usually small. The physical origin for Φ is mainly the magnetic dipole–dipole interaction. Since the dominant antisymmetric anisotropic term is from the spin–orbit coupling [1, 3], which we treat separately (cf. (1)), we can neglect $\boldsymbol{T}_{AV}$ in expression (8). It is not clear that in general one can also neglect the symmetric tensor Φ. However, in this paper we will consider only the anisotropy from spin–orbit interaction, i.e. the case $\boldsymbol{T}_{ex} = \frac{1}{3}\mathrm{tr}\,\boldsymbol{T}_{ex} = T_{IS}$.

In order to make contact with spin-polarised band calculations, we introduce the local-spin-density approximation and follow the von Barth and Hedin [14] expansion of the exchange correlation potential $V_{xc}(n(r))$ to first order in the difference of majority and minority spins $n^{\alpha}(\boldsymbol{r})$ and $n^{\beta}(\boldsymbol{r})$, yielding

$$V_{xc}(n(\boldsymbol{r})) = \mu_{xc}(n(\boldsymbol{r})) + A(n(\boldsymbol{r}))\{[n^{\alpha}(\boldsymbol{r}) - n^{\beta}(\boldsymbol{r})]/n(\boldsymbol{r})\}. \tag{9}$$

Here $\mu_{xc}(n(\boldsymbol{r}))$ and $A(n(\boldsymbol{r}))$ are independent of the spins and are related to the chemical potential of an electron gas. If we adapt (9) to the exchange potential $\boldsymbol{T}_{ex} = T_{IS}$ defined above, we can write T_{IS} as a product of an effective local potential $V_{ex}(\boldsymbol{r}) = -A(n(\boldsymbol{r}))$ with the period of the lattice and the fraction spin density $S(\boldsymbol{r}) = [n^{\alpha}(\boldsymbol{r}) - n^{\beta}(\boldsymbol{r})]/n(\boldsymbol{r})$ (in principle incommensurate with the lattice):

$$T_{IS} = -V_{ex}(\boldsymbol{r})S(\boldsymbol{r}). \tag{10}$$

By using (10) and (7) in (3), we obtain the following exchange operator expressed in fundamental quantities

$$\mathcal{H}_{ex} = -\frac{1}{2}\sum_{k,k',q}\sum_{s,s',s'',s'''}\langle s''|\sigma_1|s\rangle\langle (k-q)s'', (k'+q)s'''|V_{ex}(r)S(r)|ks, k's'\rangle$$
$$\times \langle s'''|\sigma_2|s'\rangle a^+_{(k'+q)s'''}a^+_{(k-q)s''}a_{ks}a_{k's'}. \tag{11}$$

The last term in (1) is the spin–orbit operator [15]

$$\mathcal{H}_{so} = \frac{-i\hbar}{4m^2c^2}\sum_{s,s'}\sum_{k}\langle ks|\nabla V(r)\times\nabla]\cdot\sigma|ks'\rangle a^+_{ks}a_{ks'} = \sum_{s,s'}\sum_{k}\boldsymbol{L}_k\cdot\langle s|\sigma|s'\rangle a^+_{ks}a_{ks'} \tag{12}$$

where

$$\boldsymbol{L}_k = \frac{-i\hbar}{4m^2c^2}\int \psi_k(r)^*[\nabla V(r)\times\nabla]\psi_k(r)\,dr.$$

This implies that $\mathcal{H}_{so}$ is an anisotropic operator.

By expanding the sum over the spins in (12) one obtains

$$\mathcal{H}_{so} = \sum\begin{pmatrix} L_{kz} & L_{k-} \\ L_{k+} & L_{kz}\end{pmatrix}a^+_k a_k \tag{13}$$

where a matrix element $A_{ss'}$ corresponds to the probability to have an excitation between spin states s and s'. Obviously (13) is not diagonal. However, since the matrix has the eigenvalues $\pm L_k$ one easily get the following expression for diagonalised $\mathcal{H}_{so}$:

$$\mathcal{H}_{so} = \sum_{s}\sum_{k} sL_k c^+_k c_k \tag{14}$$

where

$$L_k = (L^2_{kx} + L^2_{ky} + L^2_{kz})^{1/2}.$$

The diagonalised operator basis c_{ks}, c^+_{ks} is related to a_{ks}, a^+_{ks} by the unitary matrix $\mathbf{U}_k$ in the following way:

$$a_{ks} = (\mathbf{U}^{-1}_k)_{ss'}c_{ks} \tag{15a}$$

$$a^+_{ks} = (\mathbf{U}_k)_{s's}c^+_{ks} \tag{15b}$$

where $s \neq s'$ and

$$\mathbf{U}_k = i[2L_k(L_k + L_{kz})]^{-1/2}\begin{pmatrix} L_{k+} & -(L_k + L_{kz}) \\ L_k + L_{kz} & L_{k-}\end{pmatrix} \tag{16a}$$

$$\mathbf{U}^{-1}_k = -i[2L_k(L_k + L_{kz})]^{-1/2}\begin{pmatrix} L_{k-} & L_k + L_{kz} \\ -(L_k + L_{kz}) & L_{k+}\end{pmatrix}. \tag{16b}$$

In order to make the structure and the physical significance of the exchange part of the Hamiltonian more clear, we introduce an exchange field defined by

$$\boldsymbol{H}^{ex}_{G,i}(q) = \frac{1}{\mu_B}\sum_{G'} S_{G-G',i}(q)V_{ex,G'}. \tag{17}$$

By using (11), (14), (15) and (17) we can now obtain the Hamiltonian (1) in diagonalised form for a band system:

$$\mathcal{H}_0 + \mathcal{H}_{so} = \sum_{s}\sum_{k}(\varepsilon_k + sL_k)c^+_{ks}c_{ks} \tag{18}$$

$$\mathcal{H}_{ex} = -\mu_B \sum_{\substack{\mu,\mu' \\ \mu'',\mu'''}} \sum_{\substack{s,s' \\ s'',s'''}} \sum_{G} \sum_{k,k',q} F_G(k,k',k-q,k'+q)_{\mu\mu'\mu''\mu'''} \langle s''|\mathbf{U}_{k-q}\sigma_1\mathbf{U}_k^{-1}|s\rangle$$

$$\times \boldsymbol{H}_G^{ex}(q)\langle s'''|\mathbf{U}_{k'+q}\sigma_2\mathbf{U}_{k'}^{-1}|s'\rangle c^+_{(k+q)s'''}c^+_{(k-q)s''}c_{k's'}c_{ks}. \tag{19}$$

Here μ, μ', μ'' and μ''' are the band indices. In (19) we have utilised the following Fourier transform and the fact that the wavefunctions are of Bloch type, i.e.

$$F_G(k,k',k-q,k'-q)_{\mu\mu'\mu''\mu'''} = \sum_{G',G''} U^*_{k-q+G+G',\mu''} U^*_{k'+q+G+G'',\mu'''} U_{k+G,\mu} U_{k'+G,\mu'} \tag{20}$$

$$U_k(r) = \sum_G U_{k+G}\, e^{iG\cdot r} \tag{21}$$

$$V_{ex}(r) = \sum_g V_{ex,G}\, e^{iG\cdot r} \tag{22}$$

$$S(r)_i = \sum_G \sum_q S_{G,i}(q)\, e^{i[q\cdot(R_n+\rho)+\rho\cdot G]}. \tag{23}$$

In (23) ρ is the position in a unit cell for the electron and the index $i = x, y, z$.

3. Wavevector-dependent spin susceptibility in a two-band system

3.1. Basic theory

Since time- and space-varying magnetic fields are generally quite small in magnetically ordered systems, a linear response theory is usually adequate [16]. If the band electrons act as a liner medium, the susceptibility is independent of the effective magnetic field, and we may write [16]

$$\boldsymbol{S}_{G,i}(q) = 2\mu_B \sum_{G'} \sum_j \chi(q)^*_{GG',ij} \boldsymbol{H}^{eff}_{G',j}(q). \tag{24}$$

The corresponding exchange energy is

$$\langle \varepsilon_{ex} \rangle = -\mu_B \sum_{G,G'} \sum_q \boldsymbol{H}^{eff}_g(q) \cdot \boldsymbol{S}^*_{G'}(q). \tag{25}$$

The expectation value of the exchange energy can also be written (cf. (19))

$$\langle \varepsilon_{ex} \rangle = \frac{\mu_B}{2} \sum_{\substack{\mu,\mu' \\ \mu'',\mu'''}} \sum_{\substack{s,s', \\ s'',s'''}} \sum_{G} \sum_{k,k',q} F_G(k,k',k-q,k'+q)_{\mu\mu'\mu''\mu'''} \langle 0|c^+_{k-q}c_k|0\rangle$$

$$\times \langle s''|\mathbf{U}_{k-q}\sigma_1\mathbf{U}_k^{-1}|s\rangle \boldsymbol{H}^{ex}_G(q)\langle 0|c^+_{k'+q}c_{k'}|0\rangle\langle s'''|\mathbf{U}_{k'+q}\sigma_2\mathbf{U}_{k'}^{-1}|s''\rangle. \tag{26}$$

If $\boldsymbol{H}^{eff}$ in (25) is equal to $\boldsymbol{H}^{ex}$ defined in (17), we can here identify the spin density defined in (25) as

$$\boldsymbol{S}^*_G(q) = \frac{1}{2\Omega} \sum_{\substack{\mu,\mu', \\ \mu'',\mu'''}} \sum_{\substack{s,s', \\ s'',s'''}} \sum_{G} \sum_{k,k',q} F_G(k,k',k-q,k'+q)_{\mu\mu'\mu''\mu'''} \langle 0|c^+_{k-q}c_k|0\rangle$$

$$\times \langle s''|\mathbf{U}_{k-q}\sigma_1\mathbf{U}_k^{-1}|s\rangle\langle 0|c^+_{k'+q}c_{k'}|0\rangle\langle s'''|\mathbf{U}_{k'+q}\sigma_2\mathbf{U}_{k'}^{-1}|s'\rangle. \tag{27}$$

Here Ω is unit volume. By treating $\mathcal{H}_{ex}$ (i.e. (19)) as a perturbation on $\mathcal{H}_0$ we obtain the wavefunction of the ground state in (27) up to first order. We can then calculate the

expectation value of $S_G^*(q)$ and by using (24) we recognise the tensor expression for the susceptibility defined above:

$$\chi(q)_{GG',ij} = \chi(q)^{\mathrm{d}}_{GG'}\delta(i,j) + \chi(q)^{\mathrm{nd}}_{GG',ij} + \chi(q)^{\mathrm{so}}_{GG'}\delta(i,j). \tag{28}$$

Here

$$\chi(q)^{\mathrm{d}}_{GG'} = \sum_{k,k'} F_G(k,k',k-q,k'-q)F_{G'}(k,k',k-q,k'-q)^* \times \frac{f(\varepsilon_{\mathrm{F}}-\varepsilon_k)f(\varepsilon_{\mathrm{F}}-\varepsilon_{k'})f\varepsilon_{k-q}-\varepsilon_{\mathrm{F}})f(\varepsilon_{k'+q}-\varepsilon_{\mathrm{F}})}{\varepsilon_{k-q}+\varepsilon_{k'+q}-\varepsilon_k-\varepsilon_{k'}} \tag{29}$$

and

$$\chi(q)^{\mathrm{nd}}_{GG',ij} = \sum_{\substack{s,s',\\ s'',s'''}} \sum_{k,k'} \Lambda_{GG',ss's''s'''}(k,k',k-q,k'-q)\langle s''|\mathbf{U}_{k-q}\sigma_{1_i}\mathbf{U}_k^{-1}|s\rangle \times \langle s|\mathbf{U}_k\sigma_{1_j}\mathbf{U}_{k-q}^{-1}|s''\rangle\langle s'|\mathbf{U}_{k'}\sigma_{2_i}\mathbf{U}_{k'+q}^{-1}|s'''\rangle\langle s'''|\mathbf{U}_{k'+q}\sigma_{2_j}\mathbf{U}_{k'}^{-1}|s'\rangle \tag{30}$$

where

$$\begin{aligned}\Lambda_{GG',ss'ss''s'''}(k,k',k-q,k'-q) &= (\mu_{\mathrm{B}}/\Omega)F_G(k,k',k-q,k'-q)F_{G'}(k,k',k-q,k'-q)^* \\ &\times [f(\varepsilon_{\mathrm{F}}-\varepsilon_k+sL_k)f(\varepsilon_{\mathrm{F}}-\varepsilon_{k'}+s'L_{k'}) \\ &\times f(\varepsilon_{k-q}-s''L_{k-q}-\varepsilon_{\mathrm{F}})f(\varepsilon_{k'+q}-s'''L_{k'+q}-\varepsilon_{\mathrm{F}}) \\ &\times (\Delta\varepsilon_0+s''L_{k-q}+s'''L_{k'+q}-sL_k-s'L_{k'})^{-1} \\ &- f(\varepsilon_{\mathrm{F}}-\varepsilon_k)f(\varepsilon_{\mathrm{F}}-\varepsilon_{k'})f(\varepsilon_{k-q}-\varepsilon_{\mathrm{F}})f(\varepsilon_{k'+q}-\varepsilon_{\mathrm{F}})/\Delta\varepsilon_0].\end{aligned} \tag{31}$$

Here $f(x)$ is the Fermi function, i.e. $f(x) = 1$ for $x > 0$ and 0 for $x < 0$ when $T = 0$. Further ε_{F} is the Fermi energy, $\Delta\varepsilon_0 = \varepsilon_{k-q} + \varepsilon_{k'+q} - \varepsilon_{k'} - \varepsilon_{k'}$. In general the states k, k', $k-q$ and $k'+q$ belong to different bands. For brevity, however, the band indices have been suppressed in the expressions above. We find that χ has two diagonal terms, one (χ^{d}) from the exchange interaction and one from the spin–orbit coupling (χ^{so}). The non-diagonal contributions (χ^{nd}) arise from the exchange interaction but also indirectly from the spin–orbit interaction via the matrix $\mathbf{U}_k$ given by (16). The explicit expression for χ^{so} can be found in [17]. In (30), the summation is over all spin states that conserve the initial spins ($s + s' = s'' + s'''$).

By using expressions (17) and (24) in (25) and adding the spin–orbit energy, one gets the total magnetic energy

$$\varepsilon_{\mathrm{mag}}(q) = \sum_G \sum_{i,j} V_{\mathrm{ex},G}V^*_{\mathrm{ex},G}S_{G,i}(q)\chi(q)^{-1}_{GG',ij}S^*_{G,j}(q) + \sum_{s,s',s'',s'''}\sum_{k,k'} sL_k + s'L_{k'} + s''L_{k-q} + s'''L_{k'+q}. \tag{32}$$

One may therefore, by studying the susceptibility expressions (29)–(31), observe that (32) in fact is a linear function of χ since the spin components are proportional to χ (see (24)) and get some ideas about the origin of incommensurate magnetic structures.

For a band crossing the Fermi level, the energy denominator goes to zero for transitions with $q = 0$ within that band and consequently the susceptibility has a peak

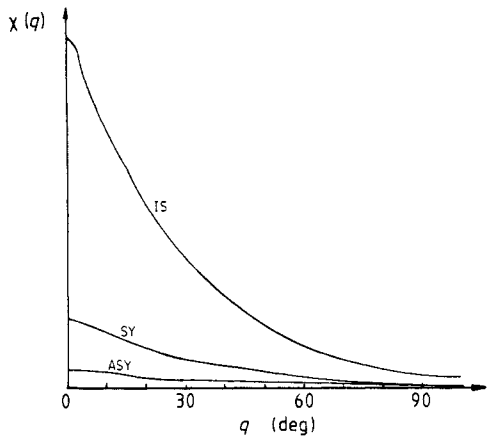

Figure 1. Results from the numerical calculations of the isotropic (IS), symmetric anisotropic (SY) and antisymmetric anisotropic (ASY) contributions to the susceptibility as a function of q, for two flat bands (one below and one above ε_F) at $T \simeq 0$. Here χ is presented in relative units and q is expressed by the rotation angle for a helix by assuming a crystal with a lattice parameter of 5 Å. The anisotropic terms correspond to a spin–orbit energy of 5% of the total energy.

for that q value. However, high magnetisation for $q \neq 0$ is also in principle a possibility for a band that intersects the Fermi surface two or more times. On the other hand, owing to the properties of the Fourier transform of e.g. a 3d or 4f orbital, the numerator is a monotonical decreasing function of q and consequently ferromagnetism seems to be favoured by all ordinary intraband transitions.

The situation is different for interband transitions since the denominators in (29) can, for $q \neq 0$, be small over an appreciable region but are in general non-vanishing for $q = 0$ transitions.

We have therefore found it worth while to study systematically the susceptibility as a function of q for two bands near to the Fermi level. In this way, we can investigate if the predicted peaks for certain q values can be reproduced for physically reasonable band structures. To do this we have simulated a number of hypothetical band structures and calculated the susceptibility numerically.

3.2. Numerical calculation of $\chi(q)$

It is too complicated to calculate the q-dependent susceptibility for incommensurate magnetic structures self-consistently through a band calculation, for example. The calculations therefore rely on a large number of sets of simulated hypothetical band structures and orbitals of 3d character. To start with, we have only calculated the dominating diagonal (isotropic) contribution, i.e. (29). In order to simplify the calculations, we have assumed that the bands are spherically symmetric and considered only two-band systems at $T = 0$.

The results show that for band structures that do not cross the Fermi surface the susceptibility curve is a monotonically decreasing function of q (figure 1). For bands that cross the Fermi surface, under certain conditions, peaks in the $\chi(q)$ curve of very variable width and amplitude can occur. More precisely, necessary but not sufficient

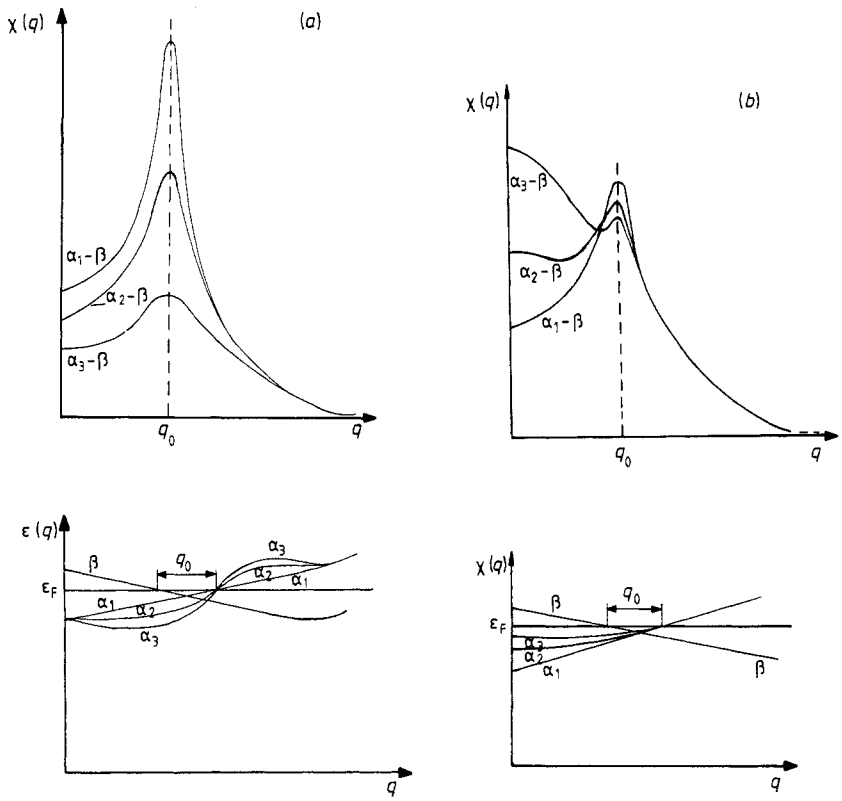

Figure 2. Results from the numerical calculations of the isotropic contributions to the susceptibility as a function of q and the corresponding band structures. This band structure type is the most favourable case for strong magnetic response at $q \neq 0$ due to interband transitions (between band β and band α_1). Notice that q_0 is equal to the distance between the intersection points of the Fermi level. (*a*) The case when the derivatives of the bands have the same magnitude but opposite sign (β and α_1) at ε_F corresponds to maximal amplitude (see text). (b) The flanks of the χ curves vary considerably with the distance of the bands to the Fermi level. Here the maximal amplitudes are almost constant since the derivative is the same at ε_F.

conditions are: (i) both bands intersect the Fermi surface at least once, (ii) narrow bands, (iii) small derivative $\mathrm{d}\varepsilon(\boldsymbol{k})/\mathrm{d}\boldsymbol{k}$ at $\boldsymbol{k} = \boldsymbol{k}_F$ and (iv) intraband transitions. We find for excitations involving two intersection points that the magnetic response can be significantly stronger for $q \neq 0$ than for $q = 0$. This result is, however, valid only for band structures of the types given in figures 2(*a*) and (*b*). On the other hand, for excitations between bands involving three different levels, we obtained no large maximum amplitude in the $\chi(q)$ curve for $q \neq 0$ (figure 3). In figures 2(*a*) and (*b*), we show examples of how a slight modification of the bands can correspond to a significant change in the shape of the $\chi(q)$ curve. One may understand this behaviour by studying the denominator of the expression (29):

$$N(\boldsymbol{k}, \boldsymbol{k}', \boldsymbol{q}) = \varepsilon_{k-q} + \varepsilon_{k'+q} - \varepsilon_k - \varepsilon_{k'}. \tag{33}$$

When $\chi(q)$ assumes its maximum value for $q = q_0 \neq 0$, it is mainly a consequence of the fact that $N(\boldsymbol{k}, \boldsymbol{k}', \boldsymbol{q})$ goes to zero. This is, however, possible only when $\boldsymbol{k}$ and $\boldsymbol{k}'$ go to $\boldsymbol{k}_F$.

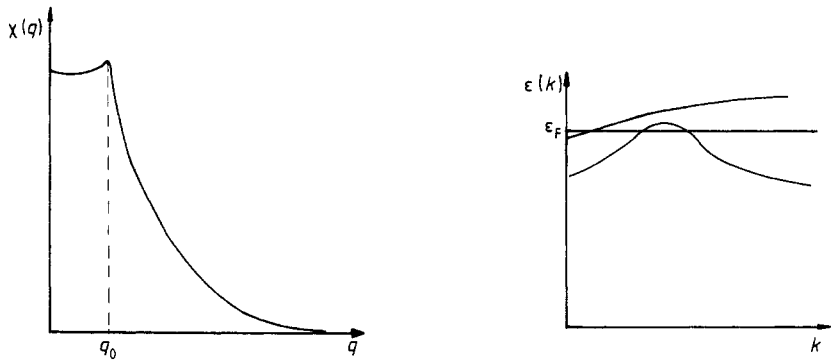

Figure 3. A typical example of a two-band structure with three intersection points of the Fermi level. The numerical calculations of this type of band structure show only a slight broadening of the χ curves in figure 1.

Furthermore a sharp peak in the $\chi(q)$ curve can occur only if $N(\boldsymbol{k}, \boldsymbol{k}', \boldsymbol{q})$ is still small for $\boldsymbol{k}$ and $\boldsymbol{k}'$ values in the neighbourhood of $\boldsymbol{k}_F$ (because the summation is performed over $\boldsymbol{k}$ and $\boldsymbol{k}'$ independently of each other). We can investigate if this is the case for the band structures in figure 2 by calculating the derivatives of $N(\boldsymbol{k}, \boldsymbol{k}', \boldsymbol{q})$ with respect to $\boldsymbol{k}$ and $\boldsymbol{k}'$. If we expand ε_k in a power series, we can keep only the linear terms (a_1, b_1, c_1 and d_1 for corresponding terms in (33)) in the neighbourhood of the minimum point (i.e. $q = q_0$) and get

$$\partial N/\partial k = a_1 - c_1 \tag{34}$$

$$\partial N/\partial k' = b_1 - d_1. \tag{35}$$

For the band structure α_1–β (in figure 2(a)) the sum of (34) and (35) is zero. The same sum is small but non-zero for α_2–β and α_3–β (in figure 2(a)), in increasing order. This holds, and this is important, also if we take into account the occupation function constraint in (29). In fact, the discussed conditions for strong peaks in the $\chi(q)$ curve are very difficult to satisfy, because they drastically limit the possible shapes and energy levels of the bands, and we have not found any bandstructure type of the two-band type other than the one given in figures 2(a) and (b) that satisfies them. According to our calculations, the conclusions above still hold if we take into consideration the single interband excitation according to Kataoka *et al* [9].

The interpretation of the numerical calculations is that topological properties of the Fermi surface is of vital importance to establish a helix of SDW.

Concerning the approximations in the calculations we may note that Umklapp processes (i.e. $G \neq 0$) have a very small influence. The same holds for the shape of the 3d orbitals. For a real and structure the k summation is performed over a Fermi surface that may deviate considerably from spherical symmetry. This affects, of course, the shape of the susceptibility curve. However, it seems reasonable that there is no qualitative difference because the properties of the Fourier transform and the mechanism for the peak in the χ curve are the same, independently of how ε varies with k.

From a mathematical point of view it is not clear that equation (29) converges for all types of bands. If all four energy levels involved are located at ε_F and moreover the Fermi surface is exactly plane for these k values, (29) may diverge or have a pole.

Table 1. The crystal symmetry of systems with magnetic helical or SDW in the ground state. The rare-earth elements Ho and Er, with the same crystal symmetry as Tm, have helical and SDW phases but their ground states have magnetic cone structures.

	Compound	Crystal structure	Space group	Inversion symmetry	Ref.
Helix	MnO_2	Tetragonal	$P4_2/mnm = D_{4h}^{14}$	Yes	[1]
	MnI_2	Trigonal	$P3m1 = D_{3d}^{3}$	Yes	[1]
	$FeCl_3$	Trigonal	$R3 = C_{3i}^{2}$	Yes	[1]
	$CsCuCl_3$	Hexagonal	$P6_122 = D_6^2$	No	[1]
	$RbFeCl_3$	HCP	$P6_3/mmc = D_{6h}^{4}$	Yes	[25]
	MnP	Orthorhombic	$Pnma = D_{2h}^{16}$	No	[18]
	FeP	Orthorhombic	$Pnma = D_{2h}^{16}$	No	[18]
	CrAs	Orthorhombic	$Pnma = D_{2h}^{16}$	No	[18]
	CoMnP	Orthorhombic	$Pnma = D_{2h}^{16}$	No	[26]
	$CrAs_{0.5}Sb_{0.5}$	Orthorhombic	$Pnma = D_{2h}^{16}$	No	[18]
	MnSi	Cubic	$P2_13 = T^4$	No	[9]
	FeGe	Cubic	$P2_13 = T^4$	No	[26]
	$MnAu_2$	?	?	?	[28]
SDW	Cr	BCC	$Im3m = O_h^9$	Yes	[2]
	Tm	HCP	$P6_3/mmc = D_{6h}^{4}$	Yes	[27]
	$HoRu_2Si_2$	Cubic	$I4 = D_{4h}^{17}$	Yes	[26]

However, it seems very improbable that band structures corresponding to large regions of an exactly plane Fermi surface can be solutions to a Schrödinger equation. We can therefore make the well founded assumption that χ is real and finite for all physically reasonable band structures.

The next step will be to take also the anisotropic term, expression (29), into account. In order to understand better how the anisotropic energy influences a helix and SDW, we will begin the next section with a symmetry analysis.

4. Symmetry analysis of a helix and a SDW

Table 1 gives 13 examples of systems with a helix structure (HS) and the only three examples of the very uncommon SDW. In table 1, a striking fact is the property that most of the crystal structures have mirror symmetry.

For HS it is also characteristic that a great number of the crystals lack inversion symmetry while all the SDW systems have inversion symmetry. Cubic symmetry seems to be under-represented in HS but not in SDW systems. Further, we see that the most frequent elements are Mn and Cr in compounds with a semiconductor (P, Si, Ge).

As has often been noticed, anisotropic exchange seems to be a determining factor for a spiral structure [1, 3, 9]. One can understand this by writing out the anisotropic terms of the magnetic energy (expression (32)):

$$\varepsilon_{\mathrm{mag}}(\boldsymbol{q}) = \sum_{G} V_{\mathrm{ex}} V_{\mathrm{ex}}^{*} (\chi_{xx}^{-1} |S_{qx}|^2 + \chi_{yy}^{-1} |S_{qy}|^2 + \chi_{zz}^{-1} |S_{qz}|^2 + \chi_{xy}^{-1} S_{qx} S_{qy}^{*} + \chi_{yx}^{-1} S_{qy} S_{qx}^{*} + \chi_{xz}^{-1} S_{qx} S_{qz}^{*} + \chi_{zx}^{-1} S_{qz} S_{qx}^{*} + \chi_{yz}^{-1} S_{qy} S_{qz}^{*} + \chi_{zy}^{-1} S_{qz} S_{q}^{*}). \tag{36}$$

For simplicity we have suppressed the reciprocal indices $\boldsymbol{G}$ in (36) (cf. (32)).

It is obvious that for a ferromagnetic structure with, say, $\boldsymbol{S}_q = S_{qx}\boldsymbol{e}_x$, all terms except the x term are zero. On the other hand for a HS in, say, the xy plane, the number of non-vanishing terms in (36) is four. This means that a HS can in principle, due to the anisotropic terms in (36), get a lower energy than a ferromagnetic configuration.

The non-diagonal matrix elements of the susceptibility tensor (or its inverse) can be separated into a symmetric ($\chi^{\mathrm{s}}_{\alpha\beta} = \chi^{\mathrm{s}}_{\beta\alpha}$; $\alpha,\beta = x, y, z$) and an antisymmetric term ($\chi^{\mathrm{as}}_{\alpha\beta} = -\chi^{\mathrm{as}}_{\beta\alpha}$):

$$\chi_{\alpha\beta}S_{q\alpha}S^*_{q\beta} + \chi_{\beta\alpha}S_{q\beta}S^*_{q\alpha} = (\chi^{\mathrm{s}}_{\alpha\beta} + \chi^{\mathrm{as}}_{\alpha\beta})S_{q\alpha}S^*_{q\beta} + (\chi^{\mathrm{s}}_{\beta\alpha} + \chi^{\mathrm{as}}_{\beta\alpha})S_{q\beta}S^*_{q\alpha}$$
$$= \chi^{\mathrm{s}}_{\alpha\beta}(S_{q\alpha}S^*_{q\beta} + S_{q\beta}S^*_{q\alpha}) + \chi^{\mathrm{as}}_{\alpha\beta}(S_{q\alpha}S^*_{q\beta} - S_{q\beta}S^*_{q\alpha}). \tag{37}$$

We will now investigate in which way relation (37) is governed by the symmetry of the spin density.

The Fourier transform of a general spin density may be written [9]

$$S(\boldsymbol{r})_\alpha = \sum_{\boldsymbol{q}}\sum_{\boldsymbol{G}} S_{\boldsymbol{G},\alpha}(\boldsymbol{q})\, \mathrm{e}^{\mathrm{i}[\boldsymbol{q}\cdot(\boldsymbol{R}_n+\boldsymbol{\rho})+\boldsymbol{\rho}\cdot\boldsymbol{G}]} \tag{38}$$

where $\boldsymbol{\rho}$ is a distance vector in a unit cell. For the special case with only one q vector and $G = 0$, (38) is reduced to

$$S_\alpha(\boldsymbol{r}) = S_{\alpha q}\,\mathrm{e}^{\mathrm{i}\boldsymbol{q}\cdot\boldsymbol{r}} + S^*_{\alpha q}\,\mathrm{e}^{-\mathrm{i}\boldsymbol{q}\cdot\boldsymbol{r}} = S_{1\alpha q}\cos(\boldsymbol{q}\cdot\boldsymbol{r}) + S_{2\alpha q}\sin(\boldsymbol{q}\cdot\boldsymbol{r}) \tag{39}$$

where

$$\boldsymbol{r} = \boldsymbol{R}_n + \boldsymbol{\rho}$$

and

$$S_{1q} = S_q + S_{-q} = S_q + S^*_q = 2\,\mathrm{Re}\,S_q \tag{40}$$

$$S_{2q} = \mathrm{i}(S_q - S_{-q}) = -2\,\mathrm{Im}\,S_q. \tag{41}$$

From the symmetry point of view, the restriction to $G = 0$ is not critical since all the terms in the reciprocal-lattice sum in (38) have the same point-group symmetry.

We will assume that a simple type of helix is given by [18]

$$S_q = \tfrac{1}{2}(\boldsymbol{u} + \mathrm{i}\boldsymbol{v})\,\mathrm{e}^{\mathrm{i}\Phi(q)} \tag{42}$$

where $\boldsymbol{u}$ and $\boldsymbol{v}$ are orthogonal normalised vectors and $\Phi(\boldsymbol{q}) = \boldsymbol{r}\cdot\boldsymbol{q} + \varphi_0$ (φ_0 is a phase angle. A component of S_q in (39) can thus be expressed as

$$S_{\alpha q} = \tfrac{1}{2}(u_\alpha\cos\Phi - v_\alpha\sin\Phi) + \tfrac{1}{2}\mathrm{i}(u_\alpha\sin\Phi + v_\alpha\cos\Phi). \tag{43}$$

By using (43) the spin product terms in (37) can now be written as

$$S_{\alpha q}S^*_{\beta q} + S_{\beta q}S^*_{\alpha q} = \tfrac{1}{2}(u_\alpha u_\beta + v_\alpha v_\beta) \tag{44}$$

$$S_{\alpha q}S^*_{\alpha q} - S_{\beta q}S^*_{\alpha q} = -\tfrac{1}{2}\mathrm{i}(u_\alpha v_\beta - v_\alpha u_\beta). \tag{45}$$

Because $\boldsymbol{u}$ and $\boldsymbol{v}$ are orthogonal unit vectors, (44) is (independently of the orientation of $\boldsymbol{u}$, $\boldsymbol{v}$) equal to zero for a helix in the $\alpha\beta$-plane. On the other hand, the antisymmetric expression (45) assumes its extreme value for a helix of type (42).

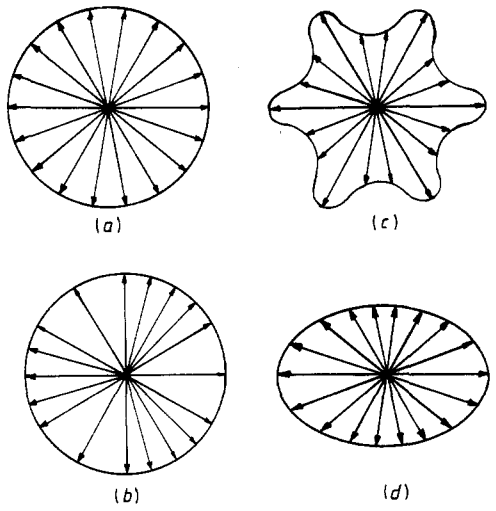

Figure 4. Schematic illustration of different types of magnetic helical structures: (*a*) isotropic circular helix; (*b*) bunched circular helix; (*c*) modulated helix; (*d*) elliptic helix. Cases (*b*)–(*d*) correspond to different anisotropic exchange energies.

For a simple SDW, as in Cr, a spin component has the form [19]

$$S_\alpha = \sum c_n \sin(\boldsymbol{q}_n \cdot \boldsymbol{r} + \Phi_n) \tag{46}$$

where the first harmonic dominates.

Contrary to the helix case, expression (46) corresponds to vanishing antisymmetric exchange (ASE) and maximum or minimum symmetric exchange (SE). A more general helical spin configuration than (38), with a modulated amplitude and/or a bunched distribution, as is illustrated in figure 4, has both SE and ASE because it may be written as a linear combination of (42) and (46).

One can experimentally determine if a helix is symmetric or antisymmetric from its dynamic spin-wave spectra [20]. The spin distribution can be measured by neutron diffraction, Mössbauer spectroscopy of nuclear magnetic resonance. This means that, if the experimental resolution is sufficiently good, one can verify if the conclusion about the space distribution of the spins is in agreement with experiment.

A natural extension of this work is thus to study the SE and ASE in more detail. The SE and ASE contributions to the susceptibility in (30) can be explicitly expressed in L_k. By using (16) and (31) and performing the summation over the spin indices for the second term in (30) under the constraint of spin conservation, one gets:

$$\begin{aligned}\chi^{\mathrm{as}}_{GG',ij}(\boldsymbol{q}) = \mathrm{i}A(i,j)\Bigg[&\sum_{\substack{\mu,\mu',\\ \mu'',\mu'''}} \sum_{k,k'} (\Lambda_{GG',1-1-11} + \Lambda_{GG',-11-11}) \\ &\times \left(\frac{L_{(k-q)_n}}{L_{k-q}} + \frac{L_{(k)_n}}{L_k}\right)\left(\frac{L_{(k'+q)_n}}{L_{k'+q}} + \frac{L_{(k')_n}}{L_{k'}}\right) \\ &+ \sum_{\substack{\mu,\mu',\\ \mu'',\mu'''}} \sum_{k,k'} (\Lambda_{GG',1111} + \Lambda_{GG',-1-1-1-1}) \\ &\times \left(\frac{L_{(k-q)_n}}{L_{k-q}} - \frac{L_{(k)_n}}{L_k}\right)\left(\frac{L_{(k'+q)_n}}{L_{k'+q}} - \frac{L_{(k')_n}}{L_{k'}}\right)\Bigg]\end{aligned} \tag{47}$$

and

$$\chi^{s}_{GG',ij}(q) = \sum_{\substack{\mu,\mu' \\ \mu'',\mu'''}} \sum_{k,k'} (\Lambda_{GG',1111} + \Lambda_{GG',-1-1-1-1} + \Lambda_{GG',1-1-11} + \Lambda_{GG',-11-11})\delta(i,j)$$

$$+ [L_{ki}L_{k'j}L_{(k-q)i}L_{(k'+q)_j} + L_{ki}L_{k'j}L_{(k-q)i}L_{(k'+q)j}$$

$$- (\boldsymbol{L}_{k-q} \cdot \boldsymbol{L}_k)(\boldsymbol{L}_{k'+q} \cdot \boldsymbol{L}_{k'})\delta(i,j)]/L_k K_{k'} L_{k-q} L_{k'+q}. \tag{48}$$

Here $A(i,j)$ is the antisymmetric operator ($A(i,j) = -A(j,i)$) and i, j, n are space coordinates x, y, z (notice that the n-coordinate in (47) is directed perpendicular to the spins).

It is obvious from (31) that the expressions (47) and (48) vanish for $L_k = 0$. As Kataoka *et al* [9] have shown, L_k vanishes for crystals with an inversion centre (neglecting relativistic effects), i.e. corresponding to a symmetric anisotropic exchange. An interesting consequence of inversion symmetry is that if a helix and a SDW of types (42) and (46), respectively, have the same isotropic energy, the SDW gets according to its collinear spin arrangement, lower anisotropic energy and consequently also lower total magnetic energy than the helix. Experimental results for Cr, $HoRu_2Si_2$ and Tm (table 1) confirm that inversion symmetry favours SDW and we have not found any counter-example. One may also note that a requirement for a contribution from the ASE expression (47) is that L_k has a component perpendicular to the plane of the helix. In a localised spin model one can show, by combining the atomic expression for the angular momentum (see, e.g., the textbook by Zieger and Pratt [21]) with the symmetry relations of the DM term (Moriya [22]), that the main component is perpendicular to the spins for crystals with a mirror plane or n-fold ($n \geq 3$) rotation symmetry (but no inversion centre). The result can give a hint of the reason why those symmetries dominate in helical systems (table 1). For itinerant magnetic systems an exhaustive investigation of expression (12) should give more information about this topic, but this is beyond scope of this paper.

5. Numerical calculation of the anisotropic susceptibility

In order to obtain an estimate of the magnitude of the symmetric and antisymmetric contributions to the susceptibility, we have numerically calculated the non-diagonal matrix elements, i.e. the expressions (47) and (48) for the band structures given in figures 1–3. The same approximations as for the diagonal terms were adapted. Unfortunately, the spin–orbit energy and the dispersion relation of L_k are complicated to calculate. We have therefore supposed that L_k is a constant. This can partly be justified by the result from orbital susceptibility calculations for 3d elements by Yasui and Shimizu [23]. The calculations have been performed for spin–orbit energies that correspond to splittings of 1%, 5% and 10% of the corresponding band energies. The result indicated that the magnitudes of the anisotropic susceptibility vary approximately linearly with the spin–orbit energy. Throughout, the symmetric terms are about a factor 2–3 larger than the antisymmetric ones and the total anisotropic contribution varies between 5 and 30% of the corresponding isotropic term (figure 1). The shapes of the curves are similar for the different contributions but somewhat flatter than the isotropic term. For example, the peaks in the anisotropic $\chi(q)$ curve have the same positions with respect to q but the half-widths are a factor 2–3 larger than in figures 2(*a*) and (*b*).

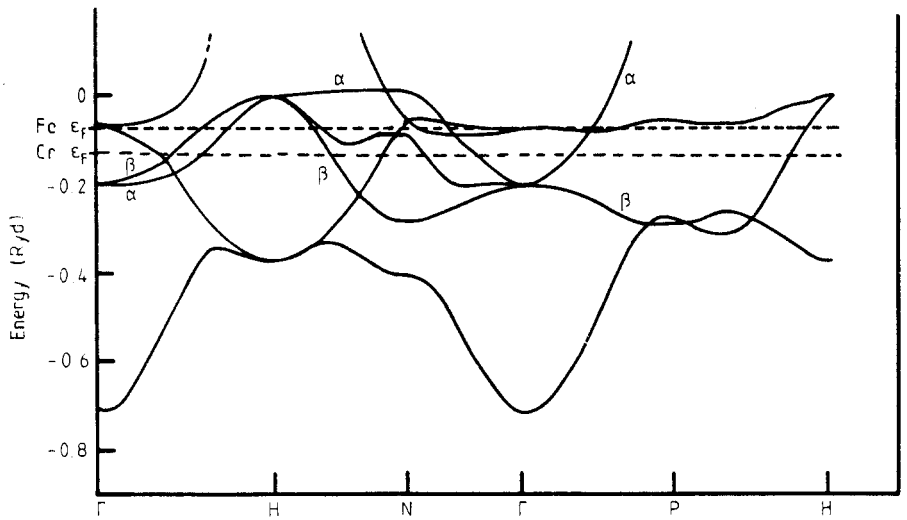

Figure 5. Non-magnetic band structures for Cr and Fe calculated by the LMTO method. The small difference in the shape between the bands of Cr and Fe has been neglected.

6. Application to Cr and MnP

Cr is the classical example of a SDW and a two-band model has been used by Fedders and Martin [7] to explain the SDW. However, their interpretation based on Lomer's [6] analysis of the Fermi surface of Cr needs to be slightly modified. Moreover, a modern band calculation gives much more accurate information about the topology of the Fermi surface.

We have therefore calculated the band structure of Cr self-consistently by the LMTO method. The atomic sphere approximation was adapted for the potential [24]. As can be seen in figure 5, four bands intersect the Fermi level. In order to demonstrate that the area of close contact between two shifted bands and the Fermi surface is large, we have sketched in figure 6 the corresponding cross sections in the (100) plane (a hole for band α around H and excess charges only around Γ for band β). As Lomer pointed out already in 1962 [6], if one shifts band α or β by $q = \pi/a \pm \varepsilon$ (ε a small number), the energy denominator in a perturbation calculation (i.e. (28) in our model) is small over an appreciable region, namely the area of contact indicated in figure 6.

The same interpretation for Fe (also BCC) gives about 50% smaller region of contact (cf. figure 6). Furthermore, analyses of the band structure of Fe and Cr show that Fe has 3d bands almost parallel with the Fermi surface, which probably favours interband transition with $q = 0$.

Manganese phosphide (MnP) has orthorhombic crystal structure with the space group P*nma* (eight atoms per unit cell) and a helical spin arrangement at low temperature which propagates in the z direction with $q = 16°$ [18]. The band structure for non-magnetic MnP has been calculated with the LMTO method. According to figure 7 this system is approximately a two-band system, of the same type as in figure 2, in the xz plane and close to the Fermi level. Band β has a hole centred around the Γ point and a small pocket of electrons between Γ and x. Band α also has a hole in the k_x–k_z plane of approximately the same shape as band β but is translated in the z direction about

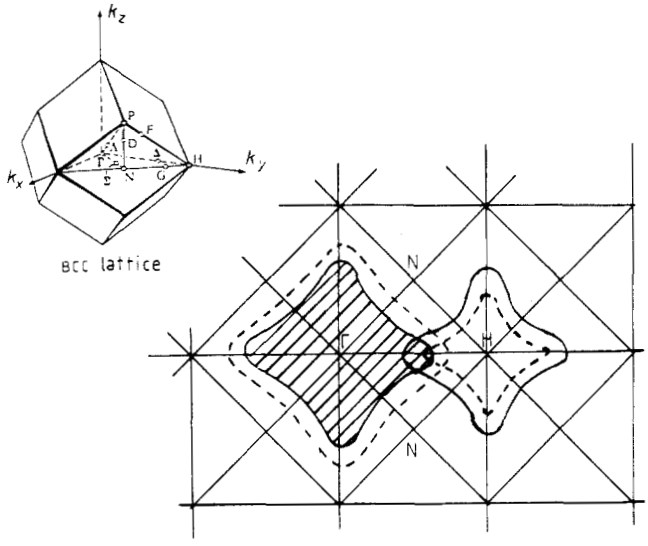

Figure 6. The cross section in reciprocal space of the (100) plane of the Fermi surface for the bands marked α and β in figure 4. Hatching indicates a separate occupied electron zone for band α in Cr. Band β has a hole around the H point marked with a full curve. The corresponding border lines are shown broken for Fe.

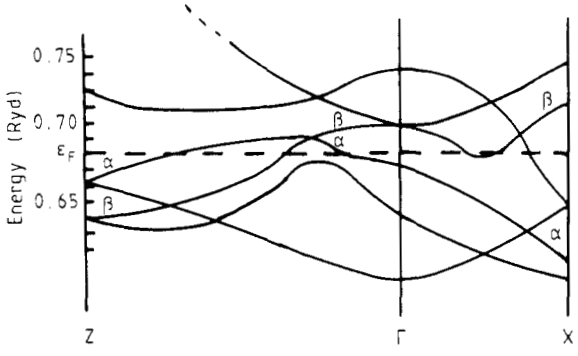

Figure 7. Part of the non-magnetic band structure for MnP, calculated by the LMTO method.

q_z = 15–65° if we assume an accuracy of ±10 mRyd in the band calculation (figure 8). It thus seems that, if the band structure is sufficiently accurately calculated, one can in the same way as for Cr qualitatively describe the occurrence of a helix and the propagation direction in terms of transitions between the bands α and β.

7. Conclusions

This work shows that, by combining perturbation theory with non-magnetic band calculations and symmetry analyses, one can get qualitative information about helimagnetism and SDW, which one cannot get from self-consistent bands or cluster calculations of large magnetic cells. The determining factor for an incommensurate magnetic structure, in the present model, is that the region of close contact between the

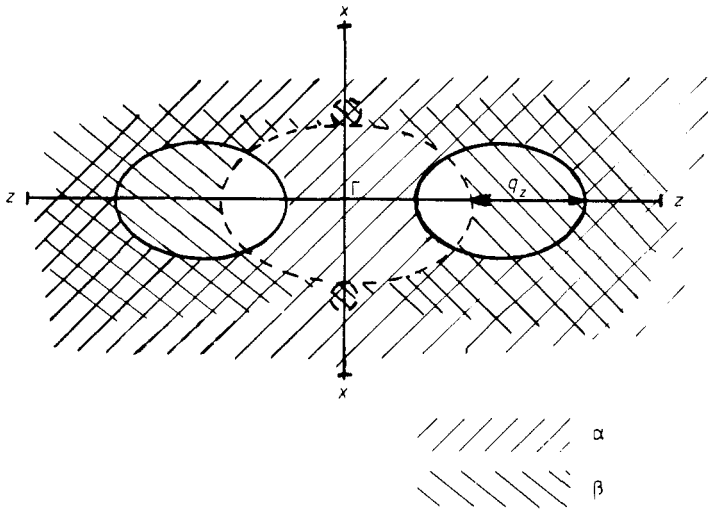

Figure 8. Sketch of the cross section in the reciprocal (101) plane of the Fermi surface for the bands marked α and β in figure 6. Hatching labels occupation of bands α and β, respectively, as shown.

q-shifted band structure and the Fermi surface is larger than for the corresponding unshifted (i.e. $q = 0$) band structure.

How powerful the approach is depends on how well the approximations introduced fit to the real system. It is doubtful, for example, if the method can be applied to systems with many bands that cross each other and the Fermi level several times. A test of this approach should be the P*n*m*a* system (to which MnP belongs). Because several helical and ferromagnetic compounds belong to this space group, one can investigate if some of the systems can be approximated by two-band systems and it is possible to determine the magnetic structure by studying transitions between two bands near to the Fermi level. By symmetry considerations of the anisotropic energy for different spin configurations, we have found that it is possible to relate the space distribution of the spins to different symmetries of the exchange energy.

Acknowledgments

I am grateful to Professor C Blomberg and Professor G Grimvall, Department of Theoretical Physics, Royal Institute of Technology, Stockholm, for reading the manuscript and suggesting several improvements. I also acknowledge Dr J-L Calais, Department of Quantum Chemistry, Uppsala University, for stimulating discussions and his contributions to the fundamental theory for section 2.

References

[1] Nagamiya T 1967 *Solid State Physics* vol 20 (New York: Academic)
[2] Carliss L, Hastings J and Weiss R 1959 *Phys. Rev. Lett.* **3** 212
[3] Bertaut E F 1963 *Magnetism* vol 3, ed G T Rado and H Suhl (New York: Academic)

[4] Overhauser A W 1962 *Phys. Rev.* **128** 1437
[5] Haman D R and Overhauser A W 1966 *Phys. Rev.* **143** 183
[6] Lomer W M 1962 *Proc. Phys. Soc.* **80** 489
[7] Fedders P A and Martin P C 1966 *Phys. Rev.* **143** 245
[8] Ukai T and Mori N 1982 *J. Appl. Phys.* **53** 2038
[9] Kataoka M, Nakanishi O, Yanase A and Kanamori J 1984 *J. Phys. Soc. Japan* **53** 3624
[10] Kübler J, Stöck K H, Sticht J and Williams A R 1988 *J. Phys. F: Met. Phys.* **18** 469
[11] You M V and Heine V 1982 *J. Phys. F: Met. Phys.* **12** 177
[12] Haimes E M, Heine V and Ziegler A 1985 *J. Phys. F: Met. Phys.* **15** 661
[13] Sandratski L M and Guletski P G 1986 *J. Phys. F: Met. Phys.* **16** L43
[14] von Barth U and Hedin L 1972 *J. Phys. C: Solid State Phys.* **5** 1629
[15] Schiff L I 1955 *Quantum Mechanics* 2nd edn (New York: McGraw-Hill) p 333
[16] White R M 1970 *Quantum Theory of Magnetism* (New York: McGraw-Hill) section 1–3
[17] Yasui M and Shimizu M 1979 *J. Phys. F: Met. Phys.* **9** 1653
[18] Kallel A, Boller H and Bertaut E F 1974 *J. Phys. Chem. Solids* **35** 1139
[19] Arrot A 1963 *Magnetism* vol 2B, ed G T Rado and H Suhl (New York: Academic)
[20] Kataoka M 1986 *J. Phys. Soc. Japan* **56** 3635
[21] Zeiger H J and Pratt G W 1973 *Magnetic Interaction in Solids* (Oxford: Clarendon)
[22] Moriya T 1960 *Phys. Rev.* **120** 91
[23] Yasui M and Shimizu M 1986 *J. Magn. Magn. Mater.* **54–57** 989
[24] Skriver H 1984 *The LMTO Method* (Berlin: Springer)
[25] Shiba H and Suzuki N 1982 *Solid State Commun.* **41** 511
[26] Oles A, Sikora W, Bombik A and Konopta L 1984 *Scientific Bulletin of the Stanislaw Statszic University of Metallurgy, Krakow* No 1005
[27] Cobblin B 1977 *The Electronic Structure of Rare-Earth Metals and Alloys* (London: Academic)
[28] Jung C H and Stoll M P H 1980 *J. Magn. Magn. Mater.* **15–18** 827